ACS APPLIED MATERIALS & INTERFACES

Research Article

www.acsami.org

Acid-Labile Poly(glycidyl methacrylate)-Based Star Gene Vectors

Yan-Yu Yang,[†,‡,§] Hao Hu,[‡,§] Xing Wang,[†] Fei Yang,[†] Hong Shen,[†] Fu-Jian Xu,*[,‡,§] and De-Cheng Wu*[,†]

[†]Beijing National Laboratory for Molecular Sciences, State Key Laboratory of Polymer Physics & Chemistry, Institute of Chemistry, Chinese Academy of Sciences, Beijing 100190, China

[‡]Key Laboratory of Carbon Fiber and Functional Polymers (Beijing University of Chemical Technology), Ministry of Education, Beijing 100029 China

[§]Beijing Laboratory of Biomedical Materials, Beijing University of Chemical Technology, Beijing 100029 China

Supporting Information

ABSTRACT: It was recently reported that ethanolamine-functionalized poly(glycidyl methacrylate) (PGEA) possesses great potential applications in gene therapy due to its good biocompatibility and high transfection efficiency. Importing responsivity into PGEA vectors would further improve their performances. Herein, a series of responsive star-shaped vectors, acetaled β-cyclodextrin-PGEAs (A-CD-PGEAs) consisting of a β-CD core and five PGEA arms linked by acid-labile acetal groups, were proposed and characterized as therapeutic pDNA vectors. The A-CD-PGEAs owned abundant hydroxyl groups to shield extra positive charges of A-CD-PGEAs/pDNA complexes, and the star structure could decrease charge density. The incorporation of acetal linkers endowed A-CD-PGEAs with pH responsivity and degradation. In weakly acidic endosome, the broken acetal linkers resulted in decomposition of A-CD-PGEAs and morphological transformation of A-CD-PGEAs/pDNA complexes, lowering cytotoxicity and accelerating release of pDNA. In comparison with control CD-PGEAs without acetal linkers, A-CD-PGEAs exhibited significantly better transfection performances.

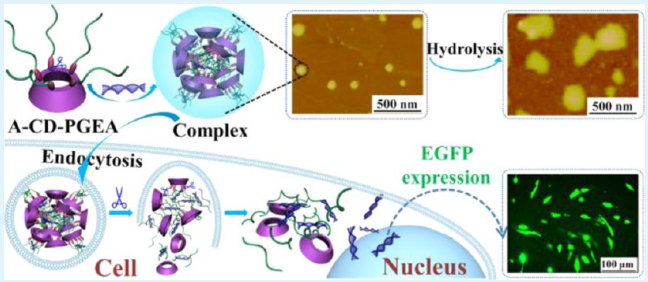

KEYWORDS: *gene vector, acetal linker, star-shaped, acid-lability, biodegradation*

INTRODUCTION

Gene therapy is a promising approach in biomedical field, where therapeutic genes can be delivered into diseased cells to cure the diseases caused by genetic abnormalities or defects.[1−4] In general, a major challenge in gene therapy is transferring genes into diseased cells due to lack of efficient biocompatible vectors. Recently, more attention was paid to nonviral gene vectors because of their low host immunogenicity, easy preparation and relative security.[5,6] Among them, polycations have been served as a dominating and promising type of nonviral gene vectors.[7,8] They can bind electronegative pDNA into complexes, which can be adsorptively endocytosized into cells followed by releasing pDNA for gene expression.[8] It was reported that polyethylenimine (PEI),[9] polyamidoamine dendrimer,[10] poly(2-dimethylamino)ethyl methacrylate (PDMAEMA),[11] and polysaccharide-based polycations[12−15] had been used as pDNA carriers. However, most of them were less biocompatible or inefficient, which gravely limited their potential applications in clinical trials. Low toxicity and high efficiency have become important criteria for designing novel and safe gene carriers.

Shielding extra charges of complexes, which can impair the effect between polycations and components in cell, is one powerful method to decrease the cytotoxicity of gene vectors.[16,17] Our group recently discovered that ethanolamine (EA)-functionalized poly(glycidyl methacrylate) (PGMA) (denoted as PGEA) possessed good gene delivery behavior in various cells.[17−19] PGEA owns massive flanking hydroxyl groups for eliminating the adverse effect of extra charges, making PGEA to be an excellent candidate for fabricating low-toxic vectors.[18−20] Designing a branched structure is deemed a valid strategy to further improve performance of gene vectors. Branched vectors can reduce the density of positive charge and further diminish the damage on cell vitality.[21−24] Our recent work indicated that high-molecular-weight comb-shaped PGEA vectors displayed much more superior biocompatibility and transfection behaviors than linear PGEA.[25]

Introduction of responsivities can impart vectors with specific ability. They can change their structures or morphologies when stimulated by glutathione (GSH), salt, or pH inside cell.[26−29] The responsive vectors can remain stable outside the cell and promote the release of pDNA under the intracellular stimulus, resulting in higher transfection activity and possible lower cytotoxicity.[30−33] β-cyclodextrin (β-CD), as a FDA-approved cyclic oligosaccharide obtained from starch,[28,29] not only can offer the biocompatible core for constructing star-shaped

Received: March 29, 2015
Accepted: May 20, 2015
Published: May 20, 2015

DOI: 10.1021/acsami.5b02733
ACS Appl. Mater. Interfaces 2015, 7, 12238−12248

Scheme 1. Preparation of (A) Acid-Labile and (B) Control PGMA-Based Star Polycations

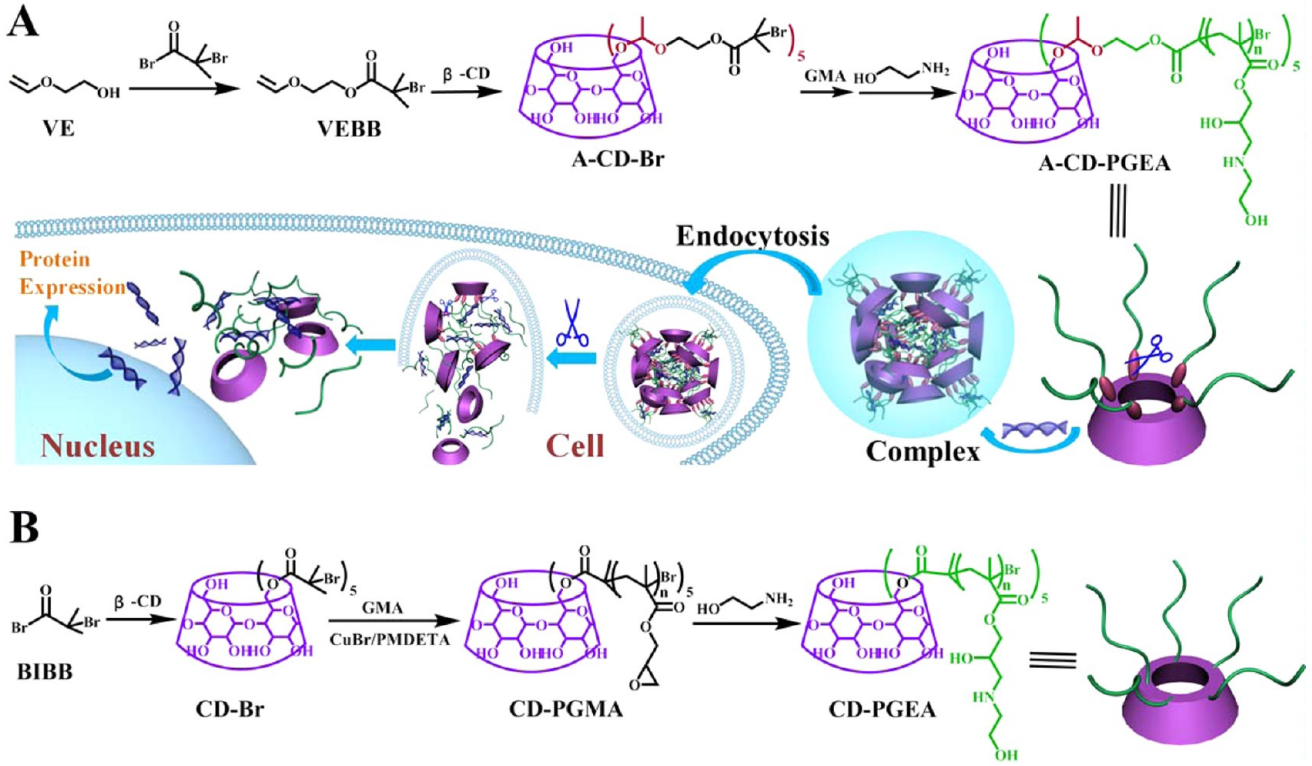

polycations, but also can enhance the ability of membrane permeation and protect the pDNA in biological media from nonspecific interactions.[15,29,34] In our previous work, a bioreducible disulfide-linked gene vector, CD-SS-PGEA, was reported, and it displayed low cytotoxicity and excellent transfection efficiency.[17] However, sensitive disulfide bridges were extremely weak and prone to breakage under alkaline environment or heating condition. During our earlier EA-modification process, disulfide bridges could barely sustain integrity under fairly mild conditions, but such a mild modification process was time-consuming and wasted almost a week. Acid-labile vector is a new focus in recent years, and diversified acid-labile groups have been incorporated into vectors, such as imine and ketal groups.[28,30−36] These acid-labile groups can be readily hydrolyzed in acidic endosome of normal cells (pH 5.5−6.5), especially in endosome of cancer cells (pH 5.0−5.5). Unlike disulfide bonds, most of acid-labile groups can remain stable under heating conditions. Compared with other acid-labile groups, acetal groups can be obtained from different kinds of hydroxyl groups, such as primary, secondary, tertiary hydroxyl groups and dihydric alcohol. In addition, the hydrolytic rate of acetal groups can be easily manipulated via altering the chemical structure of acetal groups.[28−30]

Herein, we put forward novel acid-labile acetal linkers in star-shaped PGEAs based on biocompatible β-CD cores (Scheme 1). Acetal linkers could remain intact during EA-modification step and the process could be easily achieved within an hour. The introduction of acetal linkers was capable to solve the instability of responsive bridges in sensitive PGEA vectors. Acetal linkers of the resultant pH-sensitive star PGEA (denoted as A-CD-PGEA) could be hydrolyzed under acidic endosomal environment, which was beneficial to the dissociation of pDNA within cells. A-CD-PGEAs condensed pDNA into compact complexes with high cellular uptake, and they could change morphologies in acidic endosome along with hydrolysis of acetal linkers, culminating in lower cytotoxicity and higher transfection activity.

EXPERIMENTAL SECTION

Materials. β-Cyclodextrin (β-CD, 99%), 2-(vinyloxy)-ethanol (VE, 97%), 2-bromo-2-methylpropionyl bromide (BIBB), triethanolamine (TEA), pyridinium toluene-4-sulfonate (PPTS, 98%), *N*,*N*,*N*′,*N*″,*N*′″-pentamethyl diethylenetriamine (PMDETA, 99%), copper(I) bromide (CuBr, 98%), glycidyl methacrylate (GMA, >98%), ethanolamine (EA, 98%) and branched polyethylenimine (PEI, 25 kDa) were obtained from Sigma-Aldrich Chemical Co. (St. Louis, MO). β-CD was freeze-dried before use. GMA was distilled under reduced pressure and stored at −20 °C for use. CuBr was purified by washing with acetic acid and acetone according the literature.[37] Anhydrous *N*,*N*-dimethylformamide (DMF) and dichloromethane (DCM) were obtained from a commercial solvent purification system (Innovative Technology). COS7 (African green monkey kidney fibroblast cell), C6 (rat C6 glioma cell) and HeLa (cervical cancer cell) cell lines (ATCC, Rockville, MD), plasmid pRL-CMV (pDNA) encoding Renilla luciferase (Promega Co. Cergy Pontoise, France) and plasmid enhanced green fluorescent protein (pEGFP-N1) (BD Biosciences, San Jose, CA) were used in this work. 3-(4,5-Dimethylthiazol-2-yl)-2,5-diphenyl tetrazolium bromide (MTT), penicillin, and streptomycin were purchased from Sigma-Aldrich Chemical Co.

Synthesis of 2-Vinyloxyethyl 2-Bromoisobutyrate (VEBB). VE (8.8 g, 100 mmol) and TEA (12.12 g, 120 mmol) were dissolved in 80 mL of anhydrous CH_2Cl_2 followed by cooling the solution on an ice bath for 40 min. Then, 20 mL of CH_2Cl_2 solution containing BIBB (25.8 g, 110 mmol) was slowly added, and the reaction system was allowed to warm to ambient temperature. After 5 h, CH_2Cl_2 was condensed and washed with saturated NaCl aqueous solution and deionized water three times to remove the byproducts. The organic phase was dried by anhydrous Na_2SO_4 and condensed to remove the solvent. VEBB was obtained after drying under vacuum for 2 days (yield: 22.5 g, 95%).

DOI: 10.1021/acsami.5b02733
ACS Appl. Mater. Interfaces 2015, 7, 12238−12248

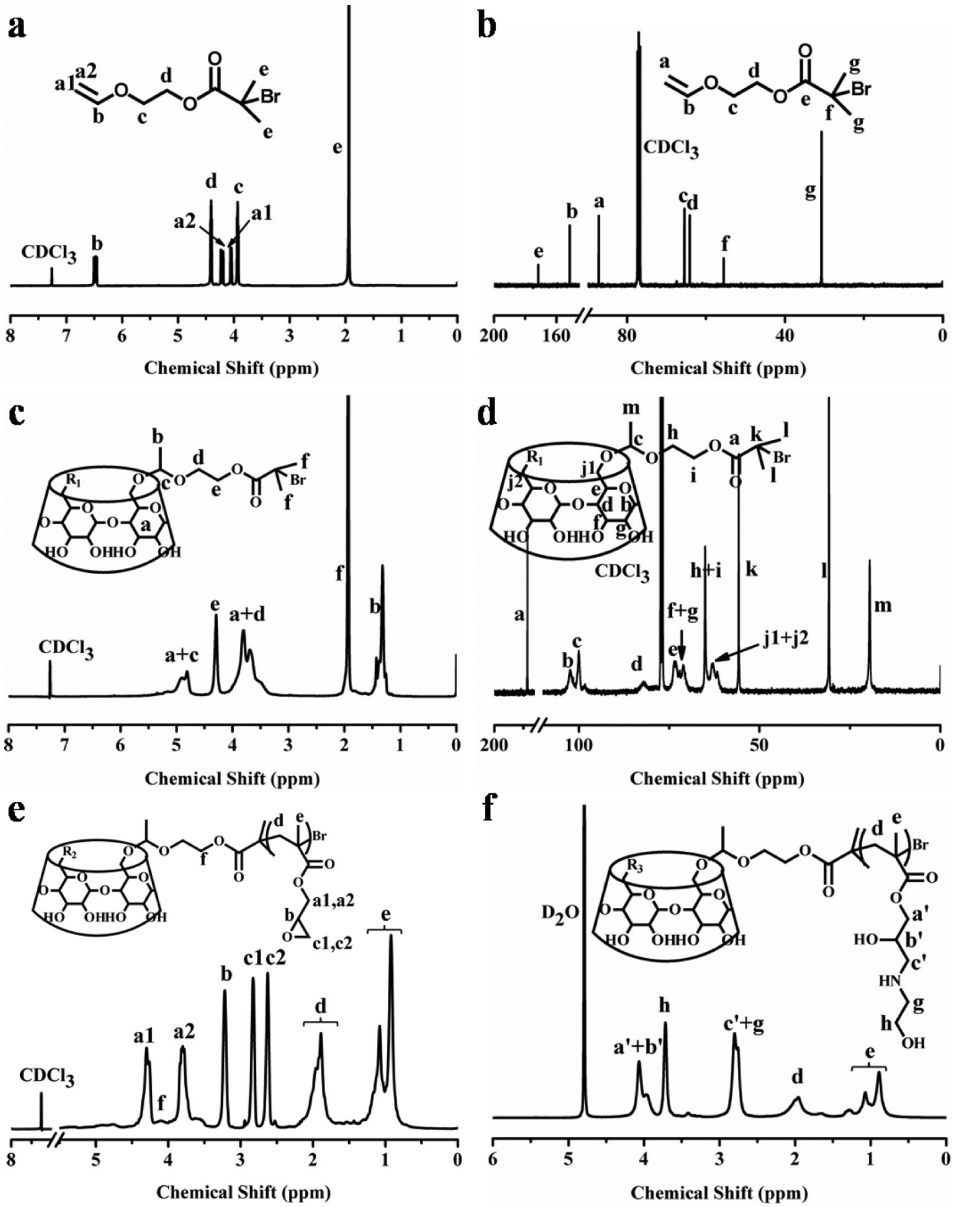

Figure 1. (a, c, e, and f) Typical ^{1}H NMR spectra and (b and d) ^{13}C NMR spectra of the intermediates and resulting polymers: (a and b) VEBB in $CDCl_3$, (c and d) A-CD-Br in $CDCl_3$, (e) A-CD-PGMA in $CDCl_3$, and (f) A-CD-PGEA in D_2O.

Synthesis of Acid-Labile β-CD-Based ATRP Initiator (A-CD-Br). β-CD (1 g, 0.88 mmol), PPTS (0.5 g, 2 mmol) and anhydrous DMSO (10 mL) were added to a two-neck round-bottom flask equipped with a constant-pressure dropping funnel containing VEBB (3.0 g, 12.6 mmol) in 5 mL of anhydrous DMSO. The reaction system was purged with argon for 20 min, prior to adding VEBB solution. After 48 h, excess K_2CO_3 was added and reaction sustained for another 2 h, meanwhile the color changed from yellow to brown. An amount of CH_2Cl_2 was added, and the organics were washed with deionized water four times. Then the organic phase was dried by anhydrous Na_2SO_4 and condensed. The crude product was repurified by precipitating into hexane three times. A-CD-Br was obtained as a brown solid after drying under vacuum (yield: 1.6 g, 80%).

Synthesis of Acid-Labile Acetaled β-CD-PGMAs (A-CD-PGMAs) and Acetaled β-CD-PGEAs (A-CD-PGEAs). A-CD-PGMAs were prepared in a 25 mL flask containing A-CD-Br initiator via ATRP using CuBr/PMDETA as catalyst systems at 30 °C. A-CD-Br (0.1 g, 0.2 equiv), GMA (3 g, 100 equiv), and PMDETA (88 μL, 2 equiv) were added to 5 mL of DMF containing 0.05 mL of highly purified water. Deoxygenation was implemented 25 min before CuBr (36 mg, 1 equiv) was added under an inert atmosphere. THF was added in the flask when the setting time arrived. Copper salts in THF solution were removed by passing through a short basic alumina column. Then, colorless THF solutions were concentrated and then precipitated in excess diethyl ether three times to obtain A-CD-PGMAs. The yields of A-CD-PGMAs at polymerization time of 0.5, 3, and 5 min were 0.28, 0.58, and 0.75 g, respectively, after drying under vacuum.

A-CD-PGEAs were obtained by postmodification with EA. 0.3 g of A-CD-PGMA and 1.5 mL of EA were added in 6 mL of DMSO followed by carrying out in an oil bath at 80 °C for 1 h. The crude products were precipitated into diethyl ether and then dialyzed against deionized water with dialysis membrane (MWCO, 3500 Da) for 20 h. A-CD-PGEAs were obtained to be white solids by freeze-drying. In the meantime, the control β-CD-PGEAs (CD-PGEAs) were also prepared. CD-PGEAs had similar structures and molecular weights to A-CD-PGEA counterparts except the acetal groups. The detailed synthetic process was illustrated in the Supporting Information.

Characterization of Polymers. Bruker DRX-400 NMR spectrometer was utilized to obtain ^{1}H and ^{13}C NMR spectra of the

DOI: 10.1021/acsami.5b02733
ACS Appl. Mater. Interfaces 2015, 7, 12238−12248

intermediates and resulting polymers. Gel permeation chromatography (GPC) was used to determine the molecular weights and molecular weight distribution of A-CD-PGMAs and A-CD-PGEAs. GPC system (Waters) was equipped with Waters-2414 refractive index detector, Waters-2487 dual wavelength (λ) UV detector and five Waters Styragel columns. THF or DMF was used as mobile phase at a flow rate of 1 mL/min at 25 °C. DMF was used as the eluent for evaluating A-CD-PGEAs in pH 5.0 acetate buffer. The molecular weights of polymers were calibrated based on polystyrene standards.

Characterization of Polymer/pDNA Complexes. The detailed preparation process of polymer/pDNA complexes and characterization techniques were described in our earlier work.[38] We prepared 0.5 mg/mL pDNA in tris-EDTA (TE) buffer and polymer solutions in highly purified water (with 10 mM nitrogen concentration) for making various complexes by mixing different amounts of polymer solution and pDNA solution homogeneously and further incubating them for 30 min. Formation and stability of the polymer/pDNA complexes were evaluated by agarose gel electrophoresis in a Sub-Cell system (Bio-Rad Laboratories). Twenty-two microliters (22 μL) of the A-CD-PGEA1/pDNA complexes was incubated in pH 5.0 acetate buffer for 4 h to measure the dissociation of pDNA from the complexes upon hydrolysis.[39] DNA bands were photographed by BioDoc-It imaging system (UVP, Inc.). The diameter and surface charge of complexes were determined by Zetasizer Nano ZS (Malvern). The morphologies of complexes before and after hydrolysis were observed on Nanoscope Multimode III AFM instrument (Veeco, Plainview, NY) in tapping mode using dry samples on mica.

Cellular Internalization. Cellular internalization was characterized by fluorescence microscope (Leica DMIL) and flow cytometry (BD LSR II, BD Biosciences, San Jose, CA). C6 cells were incubated in 24-well plate at a density of 5×10^4 cells/well for 24 h prior to transfection. YOYO-1 was used to label pDNA for 2 h before preparing different complexes. After 4 h of internalized activity, C6 cells were washed with PBS solution for five times and then imaged by fluorescence microscope. Cell nuclei were labeled by DAPI and immobilized by MeOH. For flow cytometry assay, C6 cells were seeded in 6-well plate at a density of 8×10^5 cells/well and cells were trypsinized for detection after 4 h of internalized activity.

Cell Viability. Cytotoxicity of different polycation/pDNA complexes in COS7, HeLa and C6 cell lines was evaluated by MTT assay and determined from the six wells in parallel.[38] The absorbance of each well was obtained by UV absorbance at 570 nm and the relative cell-survival percentages compared to the control (only with pDNA) were plotted against N/P ratios.

In Vitro Transfection Assay. Plasmid pRL-CMV (pDNA) and pEGFP-N1 as two kinds of reporter genes were utilized in transfection studies. Luciferase expression and EGFP expression were obtained for evaluating the transfection activity of different gene delivery system in COS7, HeLa, and C6 cell lines.[38] Luciferase expression efficiency was expressed as the protein concentration in the cells determined by bicinchoninic acid assay (Biorad Lab). The final relative light units per milligram of cell protein lysate (RLU/mg protein) were plotted against N/P ratios. EGFP expression was visible by Leica DMIL Fluorescence Microscope and the transfected cells were quantified by flow cytometry (BD LSR II, BD Biosciences, San Jose, CA).

Statistical Analysis. All tests were repeated at least three times, and the final values were expressed as average value (± standard deviation (SD)). Statistical significance was evaluated by Student's t test. P values were set less than 0.05.

RESULTS AND DISCUSSION

Preparation of Acid-Labile β-CD-Based Macro-ATRP Agent (A-CD-Br). As depicted in Scheme 1, A-CD-Br was synthesized by two steps: (1) synthesis of vinethene-containing ATRP agent (VEBB) via the reaction of BIBB with VE and (2) reaction of primary hydroxyl groups of β-CD with VEBB to produce A-CD-Br. The chemical structure of VEBB and A-CD-Br were characterized by ^{1}H and ^{13}C NMR spectra (Figure 1(a–d)). The integral area of methyl group (**e**) was double of vinyl group (**a1**, **a2**, and **b**) in Figure 1a, manifesting the vinethene group remained intact and could be modified to be acid-labile acetal linkers. For A-CD-Br, the peaks of vinyl group disappeared and the characteristic peaks of acetal group (**b**, **c** in Figure 1c and *c*, **m** in Figure 1d) appeared. The peak located at ca. δ = 1.32 ppm was attributed to the methyl group of acetal linkers (**b**, $-\underline{CH_3}$). The peak located at ca. δ = 1.88 ppm was associated with methyl group adjacent to quaternary carbon atom (**f**, $-C(Br)-(\underline{CH_3})_2$). The peaks between δ = 3.27–5.20 ppm were attributed to methylene (**d**, **e**, $-\underline{CH_2}-\underline{CH_2}-$), methyne of acetal linkers (*c*, -CH−) and carbonhydrate protons of A-CD-Br (**a**). Based on the areas of δ = 3.27–5.20 (**a**, **c**, **d**, and **e**) and of methyl group adjacent to quaternary carbon atom (**f**), the substitution degree of primary hydroxyl groups of CD was determined to be about 5.0, indicating that one A-CD-Br possessed 5 initiation sites.

Synthesis of Acid-Labile Star-Shaped Ploycations (A-CD-PGEAs). The acid-labile star-shaped A-CD-PGMAs were synthesized via ATRP from the β-CD based macro-ATRP agent, A-CD-Br. Based on the molar feed ratio [GMA]/[A-CD-Br]/[CuBr]/[PMDETA] of 100:0.2:1:2, A-CD-PGMAs with different arm lengths were prepared by using A-CD-Br at 30 °C by adjusting the polymerization time. As illustrated in Table 1,

Table 1. Characterization of the Acid-Labile A-CD-PGMAs and Control CD-PGMAs

sample	reaction time (min)	M_n (g/mol)[a]	PDI[a]	monomer repeated units per arm[b]
A-CD-Br[c]		2.4×10^3	1.07	
CD-Br[c]		1.9×10^3	1.05	
A-CD-PGMA1[d]	0.5	0.9×10^4	1.31	9
CD-PGMA1[d]	0.5	0.87×10^4	1.20	10
A-CD-PGMA2[d]	3	1.70×10^4	1.41	21
CD-PGMA2[d]	3	1.68×10^4	1.38	21
A-CD-PGMA3[d]	5	2.60×10^4	1.34	33
CD-PGMA3[d]	5	2.50×10^4	1.32	32

[a]Determined from GPC results. PDI = M_w/M_n. [b]Determined from M_n of polymers and the molecular weights of GMA (142 g/mol), A-CD-Br (2.4×10^3 g/mol) and CD-Br (1.9×10^3 g/mol). [c]A-CD-Br or CD-Br possesses five ATRP initiation sites. [d]Synthesized using a molar feed ratio [GMA]/[A-CD-Br or CD-Br]/[CuBr]/[PMDETA] of 100:0.2:1:2 at 30 °C in 5 mL of DMF/H_2O (4.95/0.05, v/v).

the number-average molecular weights (M_n) of A-CD-PGMAs with polymerization time of 0.5, 3, and 5 min were 0.9×10^4, 1.7×10^4 and 2.6×10^4 g/mol, respectively. According to the assumption that A-CD-Br possessed five ATRP initiation sites, the number of repeated GMA units per arm could be calculated to be 9, 21 and 33, respectively. In addition, the polydispersity index (PDI) from GPC data was around 1.2–1.42, indicating that the processes of ATRP were well-controlled. The acid-labile star-shaped ploycations, A-CD-PGEAs, were prepared via ring-opening reaction of A-CD-PGMAs with excess EA. EA functionalization offered one secondary amine group and two hydroxyl groups in each repeated unit of A-CD-PGEAs. The secondary amines could provide the positive charges, and the hydroxyl groups could increase the hydrophilicity of A-CD-PGEAs.

DOI: 10.1021/acsami.5b02733
ACS Appl. Mater. Interfaces 2015, 7, 12238–12248

The chemical structures of A-CD-PGMA and A-CD-PGEA were determined by ^{1}H NMR. Figure 1e displayed the typical chemical shifts attributed to GMA: **a1**, **a2** (δ = 4.31, 3.81 ppm, OCO-$\underline{CH_2}$-CH−O); **b** (δ = 3.22 ppm, $\underline{CH}$(O)−CH_2); **c1**, **c2** (δ = 2.63, 2.84 ppm, CH(O)-$\underline{CH_2}$); **d** (δ = 1.75−2.2 ppm, $C(CH_3)_2$−$\underline{CH_2}$); and **e** (δ = 0.79−1.16 ppm, C−$\underline{CH_3}$). Because of the less contribution of CD core to the overall A-CD-PGMA, the signals attributed to the carbonhydrate protons of β-CD (**f**) became much weaker. The integral area of peaks **a1** and **a2** were double that of peak **b**, manifesting that the epoxy groups were unaffected in ATRP process. After modification with EA, the peak (Figure 1e, **b**) attributed to epoxide rings of PGMA arms shifted from ca. 3.22 to 3.82−4.44 ppm, meanwhile the peaks (**c1** and **c2**) ascribed to epoxide rings of PGMA arms changed from ca. 2.84, 2.63 ppm to the same location at ca. 2.64−2.94 ppm. The integral area of methylene adjacent to hydroxyl group, **h**, was half of that of methylene groups (**g**, **c′**) adjacent to secondary amine in Figure 1f, indicating that all of epoxide rings were successfully ring-opened by EA. Number-average molecular weights of the A-CD-PGEAs were calculated according to the following equation: $M_n = M_{A\text{-}CD\text{-}Br} + (M_{GMA} + M_{EA}) \times n$, where M_n, $M_{A\text{-}CD\text{-}Br}$, M_{GMA}, and M_{EA} were molecular weights of the A-CD-PGEAs, A-CD-Br (2.4×10^3 g/mol), GMA (142 g/mol), and EA (61 g/mol), respectively, and n was the number of repeated units of corresponding A-CD-PGMAs. So, M_n of the A-CD-PGEAs were determined to be 1.18×10^4, 2.33×10^4, and 3.61×10^4 g/mol, which correspond to A-CD-PGEA1, A-CD-PGEA2, and A-CD-PGEA3, respectively.

At the same time, the control CD-PGEAs without acetal linkers were also prepared to evaluate the benefit of acetal linkers for gene delivery. As shown in Scheme 1, the control CD-PGEAs were prepared by ATRP of GMA and further modified with EA. The initiator CD-Br also had five ATRP initiation sites. The detailed procedure was described in Supporting Information. Table 1 illustrated the M_n values of CD-PGMAs were 0.87×10^4, 1.68×10^4, and 2.50×10^4 g/mol, respectively, which were similar to those of the corresponding A-CD-PGMA1, A-CD-PGMA2 and A-CD-PGMA3, respectively. Likewise, the arm lengths of CD-PGEAs were similar to those of corresponding A-CD-PGEAs. That is to say, the CD-PGEAs had semblable physiochemical properties (except acid-lability) to the acid-labile A-CD-PGEAs counterparts.

Acid-Lability of A-CD-Br and A-CD-PGEAs. Hydrolysis easily occurred in acetal groups at acidic environment, such as acetate buffer and endosome (pH 5.5−6.5) of normal cell, especially in endosome (pH 5.0−5.5) of cancer cells. Because A-CD-Br was insoluble in D_2O, hydrolysis of the A-CD-Br under acidic condition was implemented in cosolvent mixture of DMSO-d_6 and D_2O containing trace amounts of HCl for adjusting pH value to 5. As shown in Figure 2a, the peak of acetal group (1.19 ppm) disappeared completely and peaks of acetaldehyde group (2.07 and 9.59 ppm) appeared after hydrolysis. The acid-lability of A-CD-Br may provide superiority for A-CD-PGEAs on gene delivery.

A-CD-PGEAs were labile under acidic conditions, and the hydrolytic behavior could be reflected by the decrease of M_n. The GPC traces of A-CD-PGMA1 and A-CD-PGEA1 before and after hydrolysis in pH 5.0 acetate buffer are shown in Figure 2b. The elution curve of A-CD-PGEA1 presented a slightly left shift compared with that of A-CD-PGMA1. After 8 h of hydrolysis, the elution curve of A-CD-PGEA1 shifted

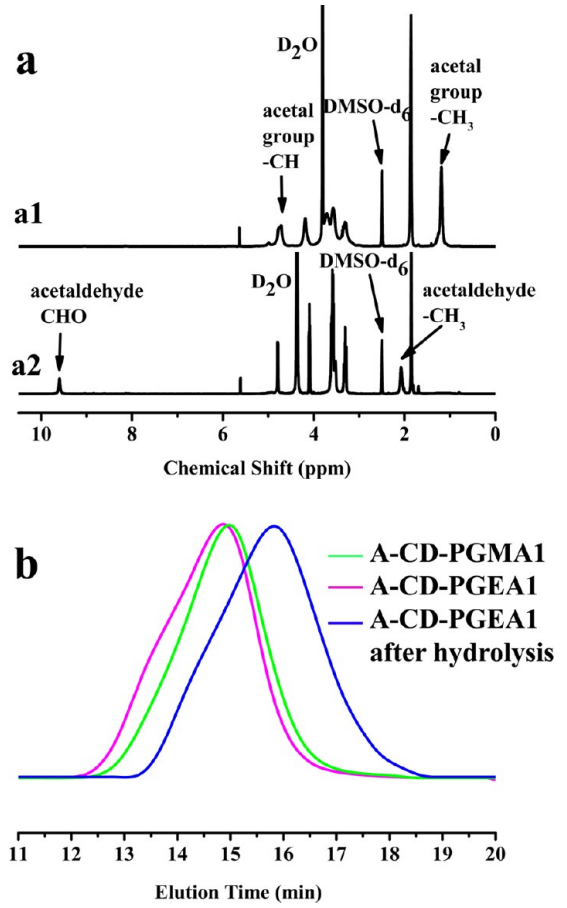

Figure 2. (a) Typical ^{1}H NMR spectra of A-CD-Br (a1) before and (a2) after incubated in pH 5 cosolvent mixture of DMSO-d_6 and D_2O containing trace amounts of HCl and (b) GPC traces of (green line) A-CD-PGMA1 and A-CD-PGEA1 (red line) before and (blue line) after incubated in pH 5.0 acetate buffer solution.

sharply toward lower molecular weight and the corresponding PDI value increased from 1.41 to 1.86. This remarkable decrease of M_n declared that hydrolysis of acetal linkers was readily performed in acidic environment. Meanwhile, it meant that A-CD-PGEAs could easily transform their structure and degrade to be straight-chain PGEA arms in acidic endosome.

Biophysical Characterization of Polymer/pDNA Complexes. Polycationic vectors can bind the negatively charged pDNA into complexes via electrostatic interaction. In this work, the formation and stability of the polycation/pDNA complexes were first evaluated by agarose gel electrophoresis shown in Figure 3. The gel retardation results confirmed that all A-CD-PGEAs and CD-PGEAs could completely retard the pDNA at N/P ratio of 1.5. To confirm the acid-lability of A-CD-PGEAs, we incubated A-CD-PGEA1/pDNA complexes as the typical example in acidic condition (pH 5.0 acetate buffer) for 4 h at 37 °C before implementing the electrophoresis assay. It was found that though A-CD-PGEA1 was protonated, hydrolyzed A-CD-PGEA1 revealed the weaker DNA binding ability (Figure 3a′). For hydrolyzed A-CD-PGEA1/pDNA complexes treated with heparin as the counter polyanion, pDNA was entirely dissociated from complexes and migrated to positive pole (Figure 3a″). However, after incubated in pH 5.0 acetate buffer and treated with heparin, the corresponding control CD-PGEA1 could still condense pDNA at higher N/P ratio (Figure 3d″). This phenomenon implied that the acid-lability of A-CD-

DOI: 10.1021/acsami.5b02733
ACS Appl. Mater. Interfaces 2015, 7, 12238−12248

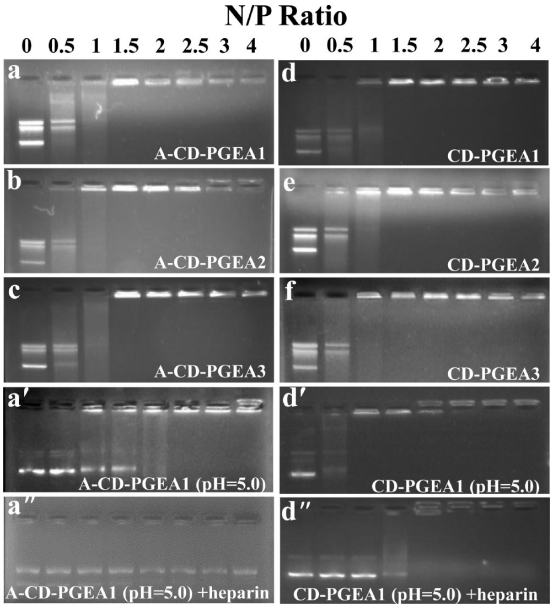

Figure 3. Agarose gel electrophoresis of (a–c) A-CD-PGEA/pDNA and (d–f) CD-PGEA/pDNA complexes at varied N/P ratios, where A-CD-PGEA1/pDNA and CD-PGEA1/pDNA complexes incubated in pH 5.0 acetate buffer in the absence (a′ and d′) and presence (a″ and d″) of the counter polyanion, heparin.

PGEAs contributed to produce unstable complexes and facilitate to release pDNA from the complexes.

The features of the polymer/pDNA complexes were also investigated by dynamic light scattering (DLS) and zeta potential. Due to their similar structures and molecular weights, A-CD-PGEA and CD-PGEA condensed pDNA into complexes with analogous characteristics. Figure 4a showed the diameter of the complexes was in the range of 100–300 nm. It is well-known that polycation/pDNA complexes are formed on account of the entanglement of polymer chains and the electrostatic interaction between polycations and electronegative pDNA. Hence, with the increase of molecular weight of A-CD-PGEAs and CD-PGEAs, the interaction of entanglement enhanced and the diameter of complexes turned smaller. Likewise, the electrostatic interaction was also reinforced with the increase of N/P ratios, therefore tending to form more compact complexes. Finally, particle sizes of polymer/pDNA complexes stabilized in the range of 100–200 nm eventually, in which complexes could readily pass through cell membranes.[40] Apart from that, A-CD-PGEA bound genes into the compact complexes, which can protect genes in extracellular environment and cytoplasm. Complexes with positive surface charges are conducive to enter cells via adsorptive endocytosis. As presented in Figure 4b, zeta potential of complexes at different N/P ratios owned a net positive surface charge of 10.7–40.25 mV and excess cationic polymer had a faint impact on surface charges of complexes at higher N/P ratios.

Hydrolysis of acetal groups incorporated into A-CD-PGEAs would affect the morphologies and sizes of the complexes. The interaction of entanglement descended along with the degradation of A-CD-PGEAs, resulting in loose complexes with larger diameters, which was confirmed by AFM and DLS. Figure 5 demonstrated the typical transformation of A-CD-PGEA2/pDNA complexes at the N/P ratio of 15 before and after treatment with pH 5.0 acetate buffer. Figure 5a displayed compact and spherical particles with the relatively uniform size

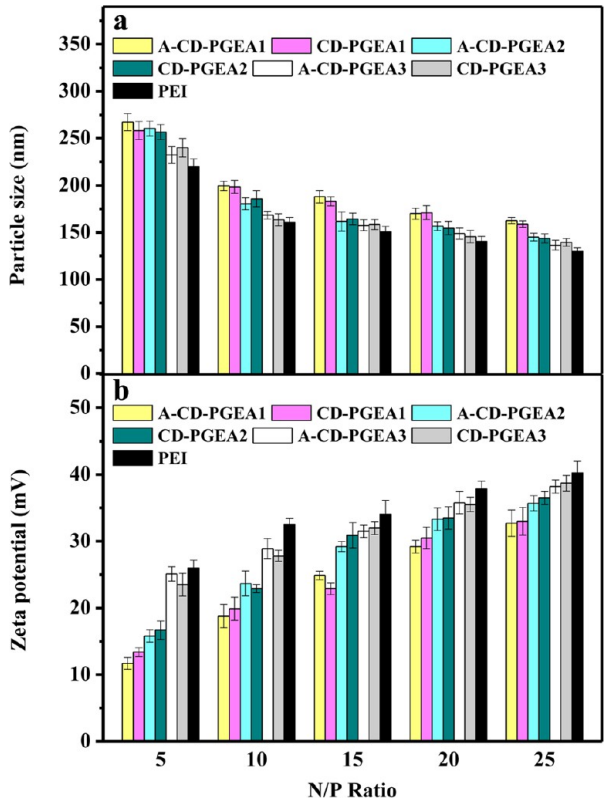

Figure 4. (a) Particle sizes and (b) zeta potentials of the complexes at different N/P ratios.

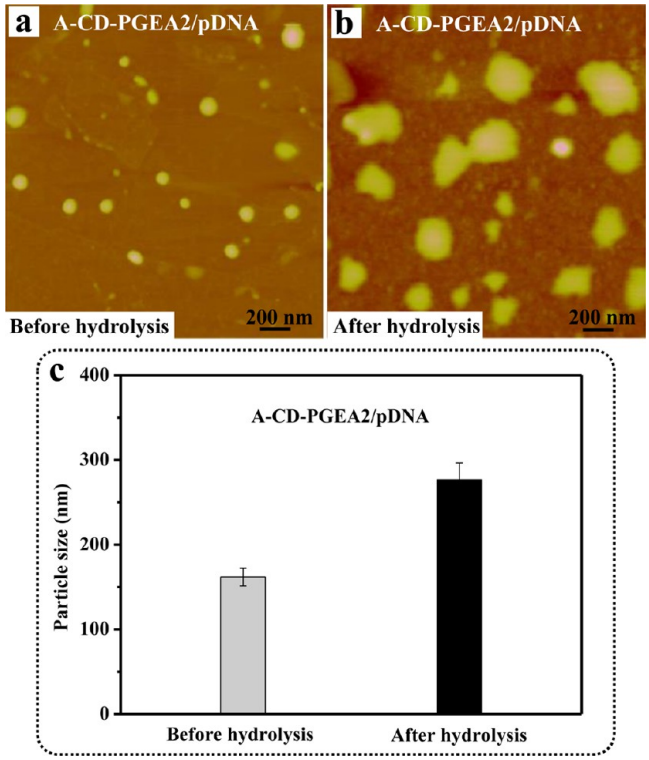

Figure 5. (a and b) AFM images and (c) particle sizes of A-CD-PGEA2/pDNA complexes at the N/P ratio of 15 before and after treatment in pH 5.0 acetate buffer solution for 8 h at 37 °C.

in the range of 100–200 nm, but loose and irregular complexes appeared (Figure 5b) after treatment in pH 5.0 solution,

DOI: 10.1021/acsami.5b02733
ACS Appl. Mater. Interfaces 2015, 7, 12238–12248

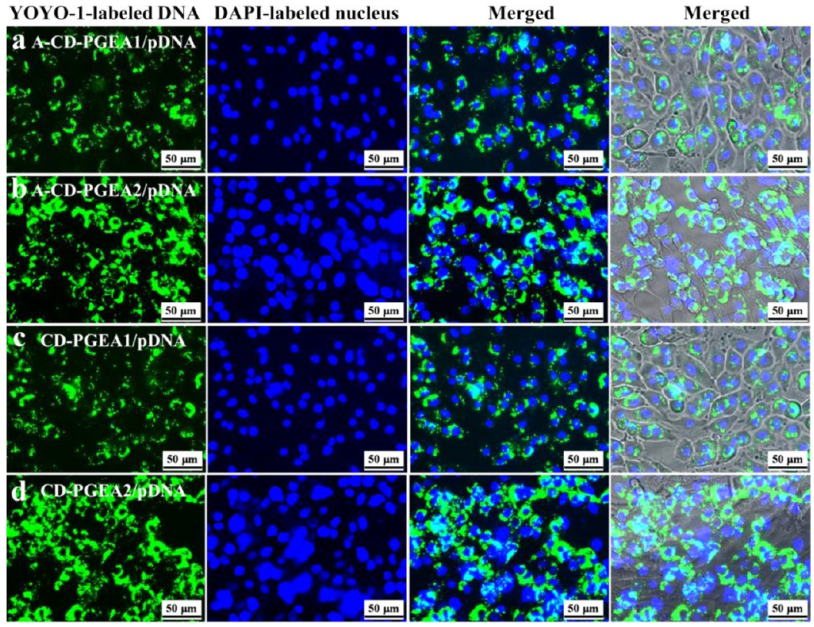

Figure 6. Fluorescent images of C6 cells treated with (a) A-CD-PGEA1/pDNA, (b) A-CD-PGEA2/pDNA, (c) CD-PGEA1/pDNA and (d) CD-PGEA2/pDNA complexes at the N/P ratio of 25. Green and blue represented pDNA labeled by YOYO-1 and nuclei labeled by DAPI.

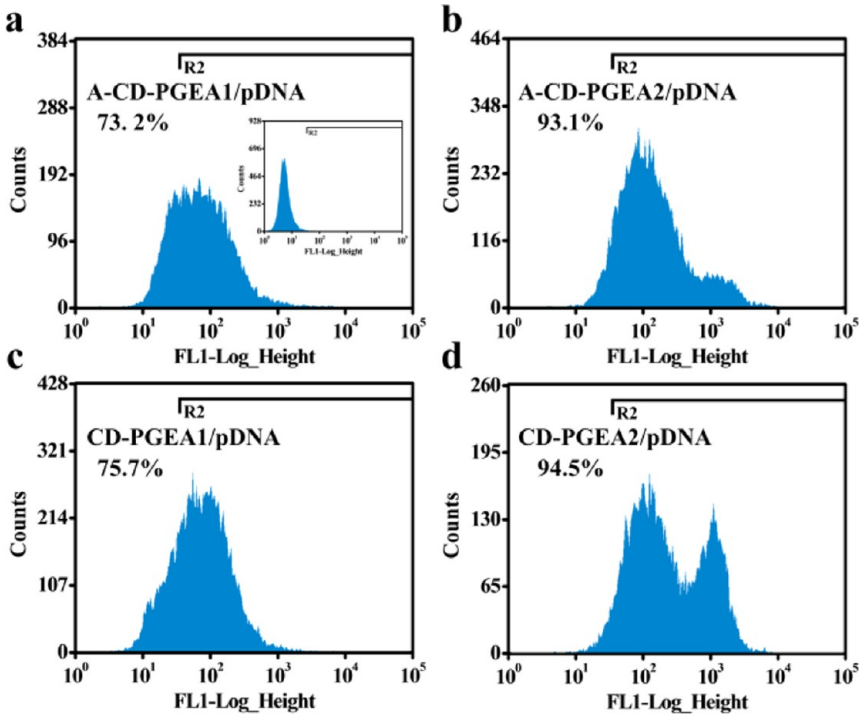

Figure 7. Flow cytometry analysis plots of C6 cells treated with (a) A-CD-PGEA1/pDNA, (b) A-CD-PGEA2/pDNA, (c) CD-PGEA1/pDNA, and (d) CD-PGEA2/pDNA complexes at the N/P ratio of 25. (a, inset) Plot ascribed to the control (untreated) C6 cells.

indicating that acetal linkers of A-CD-PGEA2 fractured. The mean size of complexes varied along with morphologic change (from 160 to 270 nm, Figure 5c). This phenomenon implied that the tight A-CD-PGEA/pDNA complexes changed to be relative loose nanoparticles after entering acidic endosome. This morphological transformation declined the binding affinity between A-CD-PGEA and pDNA, allowing pDNA to release rapidly. At the same time, hydrolysis of acetal groups and the "proton sponge effect", as well as expansion of the complexes, could cause the increase of osmotic pressure and endosomal disruption, facilitating endosomal escape of the complexes. Thus, the resultant loose complexes and rapid endosomal escape of the complexes could keep the balance between release and protection of gene during gene transfection process.

Cellular Internalization. Flow cytometry and fluorescence microscope were used to evaluate the degree of cellular internalization of different complexes. As previously reported, the complexes below 300 nm could readily enter the cell.[40] Combining with the membrane permeation-enhancing properties provided by β-CD,[15,20] A-CD-PGEA/pDNA complexes

DOI: 10.1021/acsami.5b02733
ACS Appl. Mater. Interfaces 2015, 7, 12238−12248

were endocytosized into C6 cells to a great extent, as shown in Figure 6. In addition, compact structure of complexes facilitates cellular uptake, and thus, compared with A-CD-PGEA1/pDNA complexes, more pDNA dots were observed in visual field for A-CD-PGEA2/pDNA complexes. Moreover, on account of their analogous features, A-CD-PGEA/pDNA and corresponding control CD-PGEA/pDNA complexes exhibited similar cellular uptake in fluorescence images. Flow cytometry analysis plots (Figure 7) also confirmed the above results. The internalization rate of A-CD-PGEA2/pDNA complexes was higher than A-CD-PGEA1/pDNA complexes. The consistent quantitative results of A-CD-PGEA/pDNA and control CD-PGEA/pDNA complexes are also presented in Figure 7. The higher cellular uptake of complexes provided the possibility of high gene transfection efficiency.

Cell Viability Assay. Reducing cytotoxicity must be considered in designing an effective gene delivery. In the present work, we prepared degradable A-CD-PGEAs by tailoring star-shaped PGEA and importing hydrolyzable acetal groups. The interaction of cationic vectors and basic components (cell membrane and proteins) is an important cause to cell apoptosis.[41] As reported earlier, hydroxyl groups in the repeat units of PGEAs played an important role in shielding effect for detrimental excess positive charge.[17−20] A-CD-PGEAs and CD-PGEAs with different molecular weights were much less toxic than "gold standard" PEI at varied N/P ratios in COS7, C6, and HeLa cell lines (Figure 8). MTT assay also exhibited that augment of N/P ratios and molecular weights elevated cell cytotoxicity, probably due to more redundant positive charges and stronger interaction with cell components.

At most N/P ratios (particularly higher ratios), A-CD-PGEA/pDNA complexes showed higher cell viability than corresponding control CD-PGEA/pDNA counterparts. The cytotoxicity distinctly decrease when the M_n of vectors happen to substantially reduce.[17−19] A-CD-PGEAs broke into low-molecular-weight PGEA arms along with fracture of acetal linkers in acidic endosome, where low-molecular-weight PGEA arms possessed relevantly lower cytotoxicity, tending to decrease the harmful interaction. At the highest N/P ratio of 25, the gap of cytotoxicity between A-CD-PGEA/pDNA and its counterpart was most apparent.

In Vitro Gene Transfection Assay. In vitro gene transfection efficiency of vectors was investigated by measuring the expression of luciferase and EGFP in COS7, C6, and HeLa cells. Figure 9 displays the profile of luciferase expression mediated by A-CD-PGEAs and CD-PGEAs at varied N/P ratios compared with that of PEI (25 kDa) at its optimal N/P ratio of 10 in complete serum media.[42] Gene transfection efficiency was correlated to N/P ratio of complexes and molecular weight of polycations. Augment of N/P ratio of the complexes and/or molecular weight of A-CD-PGEAs contributed to formation of the compact complexes (Figure 4a) but also slightly increased cytotoxicity (Figure 8). The compact complexes owned higher internalization rates and avoided degradation of pDNA under intracellular condition. However, the increasing cytotoxicity could cause cell death and therefore weakened the transfection activity. As a consequence, with the increase of N/P ratio, the luciferase expression mediated by low-molecular-weight A-CD-PGEA1 raised continuously, while the luciferase expression mediated by A-CD-PGEA2 and A-CD-PGEA3 presented an increase tendency at the incipient stage, and then dropped mildly.

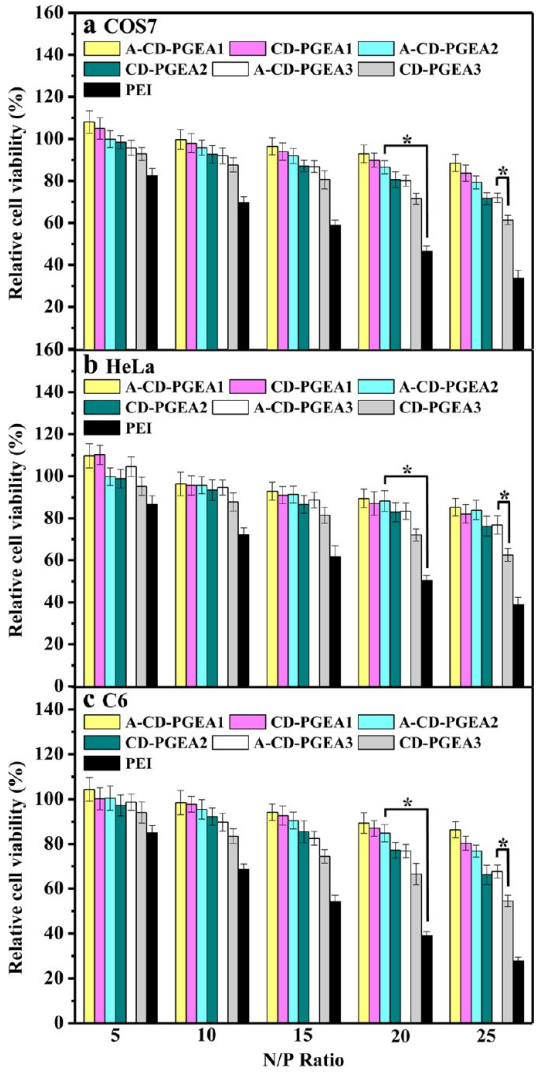

Figure 8. Cell viabilities of polymer/pDNA complexes at different N/P ratios in (a) COS7, (b) HeLa, and (c) C6 cell lines.

Transfection activity of vectors depends on the cellular uptake and the release of pDNA. High internalization rate is the premise of high efficiency, and the degree of pDNA release is a key factor to determine the transfection performance. As confirmed above (Figure 5), introduction of acetal linkers enabled A-CD-PGEA/pDNA complexes transform morphologies, therefore promoting the pDNA dissociation (Figure 3). In comparison with the control CD-PGEAs, acid-labile A-CD-PGEAs exhibited more eminent transfection behaviors, especially at higher N/P ratios (Figure 9). The distinction of gene transfection efficiency between A-CD-PGEA/pDNA and CD-PGEA/pDNA complexes was widened as molecular weight increased. In particular, A-CD-PGEA3 revealed striking difference in luciferase expression compared with its CD-PGEA3 counterpart at N/P of 25. A-CD-PGEA1 displayed mildly higher luciferase expression than its counterpart (CD-PGEA1, 1.17×10^4 g/mol) due to its inherent low transfection efficiency. In addition, difference in endosomal pH value of various cells could affect the transfection activity of acid-labile vectors,[29,30,43−45] so the gap of luciferase expression in diverse cells were also relied on the discrepant endosomal pH values of COS7 (normal cells) and C6 or HeLa cells (cancer cells). It is noted that the optimal transfection efficiency mediated by each

DOI: 10.1021/acsami.5b02733
ACS Appl. Mater. Interfaces 2015, 7, 12238−12248

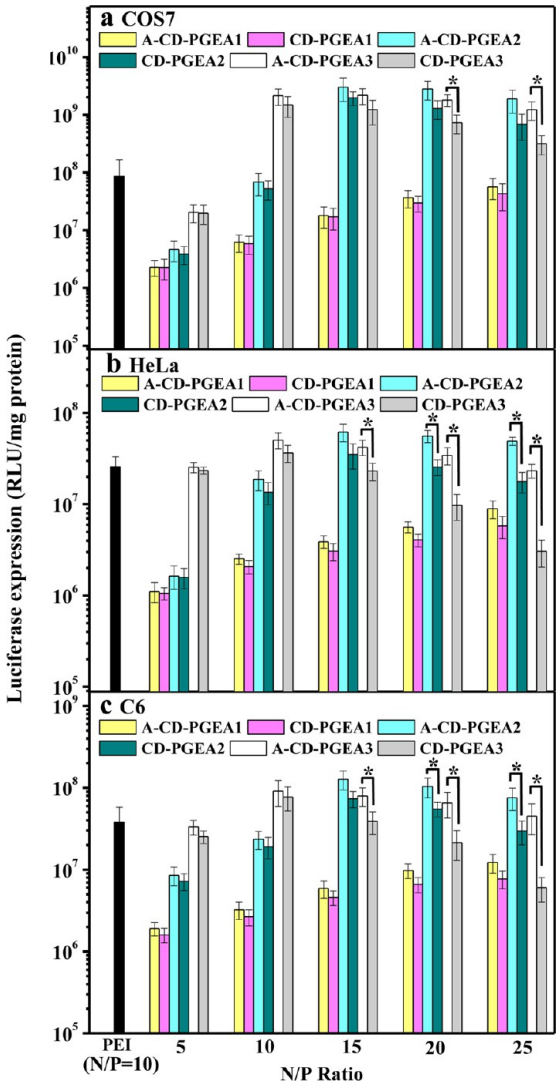

Figure 9. In vitro gene transfection efficiencies of the A-CD-PGEA/pDNA and CD-PGEA/pDNA complexes at varied N/P ratios in comparison with those of PEI (25 kDa)/pDNA complexes in (a) COS7, (b) HeLa, and (c) C6 cell lines.

A-CD-PGEA was significantly higher than that mediated by PEI.

Furthermore, EGFP expression assay was implemented to intuitively confirm the benefits of acetal linkers incorporated into A-CD-PGEAs. Figure 10 (and Figure S4, Supporting Information) shows the typical images of EGFP expression mediated by different polycation/pEGFP complexes at the N/P ratio of 25 (where A-CD-PGEAs and CD-PGEAs had biggest gap in luciferase expression, Figure 9) in C6 cells. The EGFP fluorescence signals of A-CD-PGEA/pEGFP transfection systems were stronger than those of its corresponding control CD-PGEA/pEGFP complexes. The percentages of EGFP-positive C6 cells determined by flow cytometry were 12 ± 3% and 25 ± 6% for A-CD-PGEA1 and A-CD-PGEA2, respectively, higher than those of corresponding control CD-PGEA1 (10 ± 3%) and CD-PGEA2 (17 ± 4%). The result reconfirmed the benefit of acid-labile acetal linkers to gene transfection, which was in accordance with luciferase expression assay (Figure 9).

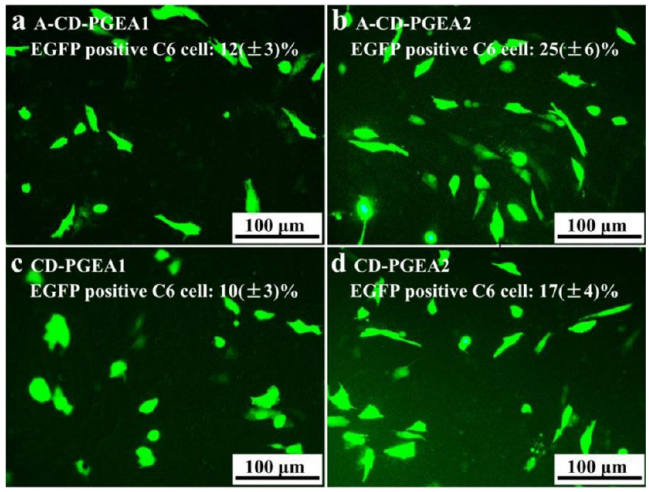

Figure 10. EGFP expression mediated by (a) A-CD-PGEA1, (b) A-CD-PGEA2, (c) CD-PGEA1, and (d) CD-PGEA2 at the N/P ratio of 25 in C6 cells.

CONCLUSION

In conclusion, a series of acid-labile A-CD-PGEA vectors were successfully prepared via incorporating the acetal bridges into star-shaped PGMA derivatives. A-CD-PGEAs could condense pDNA into the compact complexes with high cellular uptake, providing preconditions for high transfection efficiency. Along with hydrolysis of acetal linkers in acidic endosome, A-CD-PGEAs degraded into low toxic PGEA vectors. The corresponding complexes could be transformed into loose particles to facilitate pDNA release. Compared with CD-PGEAs without acetal linkers, A-CD-PGEAs demonstrated significantly better gene transfection performances. These acetal-labile star-shaped A-CD-PGEAs would provide useful information for the design of novel safe and responsive gene vectors.

ASSOCIATED CONTENT

Supporting Information

Preparation and characterization of control CD-Br, CD-PGMA, and CD-PGEA and EGFP transfection data. The Supporting Information is available free of charge on the ACS Publications website at DOI: 10.1021/acsami.5b02733.

AUTHOR INFORMATION

Corresponding Authors

*E-mail: dcwu@iccas.ac.cn.
*E-mail: xufj@mail.buct.edu.cn.

Notes

The authors declare no competing financial interest.

ACKNOWLEDGMENTS

This work was supported by NSFC (grant Nos. 21174147, 51173014, 21474115, 51221002, 51325304, and 51473014), National Young Thousand Talents Program and Collaborative Innovation Center for Cardiovascular Disorders, Beijing Anzhen Hospital Affiliated to the Capital Medical University.

REFERENCES

(1) Anderson, W. F. Human Gene Therapy. *Nature* **1998**, *392*, 25−30.
(2) Hoyer, J.; Neundorf, I. Peptide Vectors for the Nonviral Delivery of Nucleic Acids. *Acc. Chem. Res.* **2012**, *45*, 1048−1056.

DOI: 10.1021/acsami.5b02733
ACS Appl. Mater. Interfaces 2015, 7, 12238−12248

(3) Mintzer, M. A.; Simanek, E. E. Nonviral Vectors for Gene Delivery. *Chem. Rev.* **2009**, *109*, 259−302.
(4) Guo, X.; Huang, L. Recent Advances in Nonviral Vectors for Gene Delivery. *Acc. Chem. Res.* **2012**, *45*, 971−979.
(5) Yin, H.; Kanasty, R. L.; Eltoukhy, A. A.; Vegas, A. J.; Dorkin, J. R.; Anderson, D. G. Non-viral Vectors for Gene-Based Therapy. *Nat. Rev. Genet.* **2014**, *15*, 541−555.
(6) Zhang, X. F.; Tang, W. X.; Yang, Z.; Luo, X. G.; Luo, H. Y.; Gao, D.; Chen, Y.; Jiang, Q.; Liu, J.; Jiang, Z. Z. PEGylated Poly(amine-co-ester) Micelles as Biodegradable Non-viral Gene Vectors with Enhanced Stability, Reduced Toxicity and Higher in Vivo Transfection Efficacy. *J. Mater. Chem. B* **2014**, *2*, 4034−4044.
(7) Tian, H. Y.; Tang, Z. H.; Zhuang, X. L.; Chen, X. S.; Jing, X. B. Biodegradable Synthetic Polymers: Preparation, Functionalization and Biomedical Application. *Prog. Polym. Sci.* **2012**, *37*, 237−280.
(8) Ping, Y.; Wu, D. C.; Kumar, J. N.; Cheng, W. R.; Lay, C. L.; Liu, Y. Redox-Responsive Hyperbranched Poly(amido amine)s with Tertiary Amino Cores for Gene Delivery. *Biomacromolecules* **2013**, *14*, 2083−2094.
(9) Chen, D.; Ping, Y.; Tang, G. P.; Li, J. Polyethyleneimine-grafted Poly(*N*-3-hydroxypropyl) Aspartamide as a Biodegradable Gene Vector for Efficient Gene Transfection. *Soft Matter* **2010**, *6*, 955−964.
(10) Liu, H. M.; Wang, H.; Yang, W. J.; Cheng, Y. Y. Disulfide Cross-Linked Low Generation Dendrimers with High Gene Transfection Efficacy, Low Cytotoxicity, and Low Cost. *J. Am. Chem. Soc.* **2012**, *134*, 17680−17687.
(11) Yang, Y. Y.; Wang, X.; Hu, Y.; Hu, H.; Wu, D. C.; Xu, F. J. Bioreducible POSS-based Star-shaped Polymer for Efficient Gene Delivery. *ACS Appl. Mater. Interfaces* **2014**, *6*, 1044−1052.
(12) Yu, H. J.; Chen, X. S.; Lu, T. C.; Sun, J.; Tian, H. Y.; Hu, J.; Wang, Y.; Zhang, P. B.; Jing, X. B. Poly(l-lysine)-Graft-Chitosan Copolymers: Synthesis, Characterization, and Gene Transfection Effect. *Biomacromolecules* **2007**, *8*, 1425−1435.
(13) Hosseinkhani, H.; Azzam, T.; Kobayashi, H.; Hiraoka, Y.; Shimokawa, H.; Domb, A. J.; Tabata, Y. Combination of 3D Tissue Engineered Scaffold and Non-viral Gene Carrier Enhance in Vitro DNA Expression of Mesenchymal Stem Cells. *Biomaterials* **2006**, *27*, 4269−4278.
(14) Liao, Z. X.; Peng, S. F.; Chiu, Y. L.; Hsiao, C. W.; Liu, H. Y.; Lim, W. H.; Lu, H. M.; Sung, H. W. Enhancement of Efficiency of Chitosan-based Complexes for Gene Transfection with Poly(γ-glutamic acid) by Augmenting Their Cellular Uptake and Intracellular Unpackage. *J. Controlled Release* **2014**, *193*, 304−315.
(15) Ortiz-Mellet, C.; García-Fernández, J. M.; Benito, J. M. Cyclodextrin-based Gene Delivery Systems. *Chem. Soc. Rev.* **2011**, *40*, 1586−1608.
(16) Mastorakos, P.; Kambhampati, S. P.; Mishra, M. K.; Wu, T.; Song, E.; Hanes, J.; Kannan, R. M. Hydroxyl PAMAM Dendrimer-Based Gene Vectors for Transgene Delivery to Human Retinal Pigment Epithelial Cells. *Nanoscale* **2015**, *7*, 3845−3856.
(17) Hu, Y.; Zhu, Y.; Yang, W. T.; Xu, F. J. New Star-Shaped Carriers Composed of β-Cyclodextrin Cores and Disulfide-Linked Poly(glycidyl methacrylate) Derivative Arms with Plentiful Flanking Secondary Amine and Hydroxyl Groups for Highly Efficient Gene Delivery. *ACS Appl. Mater. Interfaces* **2013**, *5*, 703−712.
(18) Zhao, Y.; Yu, B. R.; Hu, H.; Hu, Y.; Zhao, N. N.; Xu, F. J. New Low Molecular Weight Polycation-Based Nanoparticles for Effective Codelivery of pDNA and Drug. *ACS Appl. Mater. Interfaces* **2014**, *6*, 17911−17919.
(19) Hu, H.; Song, H. Q.; Yu, B. R.; Cai, Q.; Zhu, Y.; Xu, F. J. A Series of New Supramolecular Polycations for Effective Gene Transfection. *Polym. Chem.* **2015**, *6*, 2466−2477.
(20) Yang, X. C.; Niu, Y. L.; Zhao, N. N.; Mao, C.; Xu, F. J. A Biocleavable Pullulan-based Vector via ATRP for Liver Cell-Targeting Gene Delivery. *Biomaterials* **2014**, *35*, 3873−3884.
(21) Kim, T. I.; Baek, J. U.; Bai, C. Z.; Park, J. S. Arginine-conjugated Polypropylenimine Dendrimer as a Non-toxic and Efficient Gene Delivery Carrier. *Biomaterials* **2007**, *28*, 2061−2067.
(22) Lakshminarayanan, A.; Ravi, V. K.; Tatineni, R.; Rajesh, Y. B. R. D.; Maingi, V.; Vasu, K. S.; Madhusudhan, N.; Maiti, P. K.; Sood, A. K.; Das, S.; Jayaraman, N. Efficient Dendrimer-DNA Complexation and Gene Delivery Vector Properties of Nitrogen-Core Poly(propyl ether imine) Dendrimer in Mammalian Cells. *Bioconjugate Chem.* **2013**, *24*, 1612−1623.
(23) Zhao, T. Y.; Zhang, H.; Newland, B.; Aied, A.; Zhou, D. Z.; Wang, W. X. Significance of Branching for Transfection: Synthesis of Highly Branched Degradable Functional Poly(dimethylaminoethyl methacrylate) by Vinyl Oligomer Combination. *Angew. Chem., Int. Ed.* **2014**, *53*, 6095−6100.
(24) Nakayama, Y. Hyperbranched Polymeric "Star Vectors" for Effective DNA or siRNA Delivery. *Acc. Chem. Res.* **2012**, *45*, 994−1004.
(25) Yang, X. C.; Chai, M. Y.; Zhu, Y.; Yang, W. T.; Xu, F. J. Facilitation of Gene Transfection with Well-Defined Degradable Comb-Shaped Poly(glycidyl methacrylate) Derivative Vectors. *Bioconjugate Chem.* **2012**, *23*, 618−626.
(26) Shima, M. S.; Kwon, Y. J. Acid-transforming Polypeptide Micelles for Targeted Nonviral Gene Delivery. *Biomaterials* **2010**, *31*, 3404−3413.
(27) Wijaya, A.; Schaffer, S. B.; Pallares, I. G.; Hamad-Schifferli, K. Selective Release of Multiple DNA Oligonucleotides from Gold Nanorods. *ACS Nano* **2009**, *3*, 80−86.
(28) Cao, H. L.; Dong, Y. X.; Aied, A.; Zhao, T. Y.; Chen, X.; Wang, W. X.; Pandit, A. Acetal-linked Branched Poly(dimethyl-aminoethyl methacrylate) as an Acid Cleavable Gene Vector with Reduced Cytotoxicity. *Chem. Commun.* **2014**, *50*, 15565−15568.
(29) Durmaz, Y. Y.; Lin, Y. L.; ElSayed, M. E. H. Development of Degradable, pH-Sensitive Star Vectors for Enhancing the Cytoplasmic Delivery of Nucleic Acids. *Adv. Funct. Mater.* **2013**, *23*, 3885−3895.
(30) Park, I. K.; Singha, K.; Arote, R. B.; Choi, Y. J.; Kim, W. J.; Cho, H. S. pH-Responsive Polymers as Gene Carriers. *Macromol. Rapid Commun.* **2010**, *31*, 1122−1133.
(31) Shim, M. S.; Kwon, Y. J. Stimuli-responsive Polymers and Nanomaterials for Gene Delivery and Imaging Applications. *Adv. Drug Delivery Rev.* **2012**, *64*, 1046−1058.
(32) Chen, W.; Meng, F. H.; Cheng, R.; Deng, C.; Feijen, J.; Zhong, Z. Y. Advanced Drug and Gene Delivery Systems Based on Functional Biodegradable Polycarbonates and Copolymers. *J. Controlled Release* **2014**, *190*, 398−414.
(33) Zhu, C. H.; Zheng, M.; Meng, F. H.; Mickler, F. M.; Ruthardt, N.; Zhu, X. L.; Zhong, Z. Y. Reversibly Shielded DNA Polyplexes Based on Bioreducible PDMAEMA-SS-PEG-SS-PDMAEMA Triblock Copolymers Mediate Markedly Enhanced Nonviral Gene Transfection. *Biomacromolecules* **2012**, *13*, 769−778.
(34) Kulkarni, A.; Deng, W.; Hyun, S. H.; Thompson, D. H. Development of a Low Toxicity, Effective pDNA Vector Based on Noncovalent Assembly of Bioresponsive Amino-β-cyclodextrin: Adamantane-Poly(vinyl alcohol)-Poly(ethylene glycol) Transfection Complexes. *Bioconjugate Chem.* **2012**, *23*, 933−940.
(35) Walker, G. F.; Fella, C.; Pelisek, J.; Fahrmeir, J.; Boeckle, S.; Ogris, M.; Wagner, E. Toward Synthetic Viruses: Endosomal pH-Triggered Deshielding of Targeted Polyplexes Greatly Enhances Gene Transfer in Vitro and in Vivo. *Mol. Ther.* **2005**, *11*, 418−425.
(36) He, H.; Bai, Y. G.; Wang, J. H.; Deng, Q. R.; Zhu, L. P.; Meng, F. H.; Zhong, Z. Y.; Yin, L. C. Reversibly Cross-Linked Polyplexes Enable Cancer-Targeted Gene Delivery via Self-Promoted DNA Release and Self-Diminished Toxicity. *Biomacromolecules* **2015**, *16*, 1390−1400.
(37) Shi, Y.; Zhu, W.; Chen, Y. M. Synthesis of Cylindrical Polymer Brushes with Umbrella-like Side Chains via a Combination of Grafting-from and Grafting-onto Methods. *Macromolecules* **2013**, *46*, 2391−2398.
(38) Xu, F. J.; Li, H. Z.; Li, J.; Zhang, Z. X.; Kang, E. T.; Neoh, K. G. Pentablock Copolymers of Poly(ethylene glycol), Poly((2-dimethyl amino)ethyl methacrylate) and Poly(2-hydroxyethyl methacrylate) from Consecutive Atom Transfer Radical Polymerizations for Non-viral Gene Delivery. *Biomaterials* **2008**, *29*, 3023−3033.

DOI: 10.1021/acsami.5b02733
ACS Appl. Mater. Interfaces 2015, 7, 12238−12248

(39) Shim, M. S.; Kwon, Y. J. Controlled Delivery of Plasmid DNA and siRNA to Intracellular Targets Using Ketalized Polyethylenimine. *Biomacromolecules* **2008**, *9*, 444−455.
(40) Nishiyama, N.; Kataoka, K. Current State, Achievements, and Future Prospects of Polymeric Micelles as Nanocarriers for Drug and Gene Delivery. *Pharmacol. Ther.* **2006**, *112*, 630−648.
(41) Kang, H. C.; Kang, H. J.; Bae, Y. H. A Reducible Polycationic Gene Vector Derived from Thiolated Low Molecular Weight Branched Polyethyleneimine Linked by 2-Iminothiolane. *Biomaterials* **2011**, *32*, 1193−1203.
(42) Wu, D. C.; Liu, Y.; Jiang, X.; He, C. B.; Goh, S. H.; Leong, K. W. Hyperbranched Poly(amino ester)s with Different Terminal Amine Groups for DNA Delivery. *Biomacromolecules* **2006**, *7*, 1879−1883.
(43) Simon, S. M. Role of Organelle pH in Tumor Cell Biology and Drug Resistance. *Drug Discovery Today* **1999**, *4*, 32−38.
(44) Lee, R. J.; Wang, S.; Low, P. S. Measurement of Endosome pH Following Folate Receptor-mediated Endocytosis. *Biochim. Biophys. Acta, Mol. Cell Res.* **1996**, *1312*, 237−242.
(45) Altan, N.; Chen, Y.; Schindler, M.; Simon, S. M. Defective Acidification in Human Breast Tumor Cells and Implications for Chemotherapy. *J. Exp. Med.* **1998**, *187*, 1583−1598.

DOI: 10.1021/acsami.5b02733
ACS Appl. Mater. Interfaces 2015, 7, 12238−12248